Stability of the Boundary Layer on a Spinning Blunt-Nosed Cylinder

Kai-Hsiung Kao* and Chuen-Yen Chow†
University of Colorado, Boulder, Colorado 80309

A linear stability analysis has been carried out by the authors (Kao, K. H., and Chow, C. Y., "Stability Analyses of Boundary Layer on a Semi-Infinite Circular Cylinder With and Without Spin," AIAA Paper 90-0116, 1990) for an incompressible laminar boundary layer along a semi-infinite cylinder of constant radius aligned with an external flow, with and without a constant angular speed about its axis. The influences of transverse curvature and spin motion are shown to have stabilizing and destabilizing effects, respectively. That work is extended here to consider a more realistic cylindrical body with a blunt nose, which generates an axial pressure gradient in the boundary layer. A numerical procedure is described to examine the stability of the boundary layer along a Rankine half-body generated by superposition of a point source and a uniform flow. Boundary-layer profiles and their neutral stability curves are obtained by the application of an implicit method and the Chebyshev collocation spectral method, respectively. From stability diagrams obtained herein for the cylinder with and without spin, the critical Reynolds number and the position on the cylinder at which onset of instability occurs can be determined.

Nomenclature

C_p = pressure coefficient
c = complex phase velocity
D = $2R_0$, diameter of the cylinder far downstream
f = nondimensional stream function
g = nondimensional velocity in the azimuthal direction
i = $\sqrt{-1}$, imaginary unit
M = pressure gradient parameter
m = strength of a point source
n = integer wave number in the azimuthal direction
O = nose point
P = space point
P = mean pressure
P' = surface point on the cylinder
p = static pressure
p' = unsteady small perturbed pressure
p_∞ = farfield pressure
R = radius parameter
R_0 = radius of cylinder far downstream
Re_D = Reynolds number based on D
Re_δ = Reynolds number based on the characteristic length δ
r = radial distance from the body axis
r_0 = distance from the surface point to body axis
$\tilde{r}_0$ = dimensional local radius
S = dimensionless spin rate
t = time
U_e = u_e/u_∞
U,V,W = mean velocities
u_e = velocity at the edge of boundary layer
u_∞ = freestream velocity
u,v,w = total velocities
u',v',w' = small perturbed velocities
V = mean velocity vector
v = total velocity vector
v' = perturbed velocity vector
x = meridian distance from the nose point
y = normal distance from the surface of cylinder
z = axial distance from the nose point
α = wave number in the meridian direction, real
Γ = meridian curve
Ω = constant angular velocity
ψ,Ψ = stream functions
ρ = density of the fluid
θ = azimuthal angle
$\xi,\eta,\zeta,\tau,\delta$ = transformed variables

Subscripts

$( )_w$ = condition on body surface
$( )_{tr}$ = value at onset of instability

Superscript

$\hat{( )}$ = complex eigenfunction

I. Introduction

THROUGH the study of flow structures in a three-dimensional boundary layer along an axisymmetric body such as a missile, one might obtain practical understanding of the flight dynamics of such a spinning or nonspinning body. However, due to its complicated nature, much still needs to be clarified about this problem, particularly with regard to the transition to a turbulent state in the boundary layer. A remarkable phenomenon connected with transition in the boundary layer occurs on blunt bodies such as spheres or circular cylinders. Transition to turbulence of a laminar boundary layer causes the point of separation on a blunt body to move downstream, which considerably decreases the width of the wake.

The fluid dynamics of a spinning body of revolution can be influenced significantly by the transverse curvature, the spin rate, the pressure gradient acting on the body, and so forth. These factors are major contributors to the dominant mechanisms for influencing flow stability. A great deal of research has been conducted to examine the effects of those parameters. For example, the experiments by Schubauer and Skramstad[2] and those by Liepmann[3] showed qualitatively that a pressure gradient had a stabilizing or destabilizing effect depending on

Presented as Paper 90-0117 at the AIAA 28th Aerospace Sciences Meeting, Reno, NV, Jan. 8-11, 1990; received Feb. 17, 1990; revision received July 19, 1990; second revision received Aug. 6, 1990; accepted for publication Aug. 15, 1990.

*Research Associate, Aerospace Engineering Sciences. Member AIAA.
†Professor, Aerospace Engineering Sciences. Associate Fellow AIAA.

whether the gradient was favorable or adverse. Many calculations have been made of the effects of pressure gradient on hydrodynamic stability. Pretsch,[4,5] Hahnemann et al.,[6] and Tetervin[7] examined the Falkner-Skan profiles. Schlichting and Ulrich[8] and Hahnemann et al.[6] improved the approximation of velocity profiles by using sixth-order polynomials. Furthermore, the combinations of sinusoidal and exponential functions for the base flow distributions were evaluated by Tetervin and Levine.[9]

Experimental investigations have been made to study the axisymmetric boundary-layer instability under the influences of spin motion and pressure gradient. Kobayashi et al.[10] were first to find the existence of spiral vortices in the boundary layer of a rotating 30-deg cone in axial flow. In the case of a sphere, Sawatzki[11] found first the vortices, and then Wirmer[12] and Kohama and Kobayashi[13] carried out further studies in detail. In 1957, Brown[14] initiated an experimental program at the University of Notre Dame to study natural transition on ogive nose cylinders aligned parallel to the flow. Thereafter, Knapp and Roache[15] studied natural and forced transitions in subsonic boundary layers in both zero and adverse pressure gradients. Kegelman et al.[16,17] made a series of wind-tunnel studies to obtain an understanding of the effects of spin on the boundary layer of secant-ogive nose axisymmetric bodies. They found that, for spin rates less than 0.4, there were no visible changes compared with the nonspinning model in the boundary-layer characteristics, with the exception of a slight skewness in the tips of the vortex trusses. A similar investigation was made by Kohama[18] on a tangent-ogive nose body. Recently, Stetson[19] was able to study the cone frustum pressure gradient effects on transition.

A theoretical investigation of transverse curvature and spin motion effects on stability of the boundary layer over a cylinder has been made by the present authors[1]; that work is extended here to study further those effects in the presence of a pressure gradient. The pressure distribution used in this analysis is taken from that on a Rankine nose cylinder rotating with a constant angular velocity about its axis in a uniform flow, which provides both favorable and adverse pressure gradients along the body surface. The favorable pressure gradient is produced in the accelerating flow region near the nose. Continuing down the body, the flow becomes faster than the freestream speed and requires an adverse pressure gradient to decelerate it back to that speed far downstream on the cylinder.

Boundary-layer flows with rotational symmetry provide simplified examples of three-dimensional flow in that they are independent of one of the space coordinates. The extension of a two-dimensional boundary layer to this type of flow was first considered by Boltz[20] and later by Millikan.[21] The boundary-layer equations were derived by Mangler[22] and are valid in regions where the principal radii of curvature of the body are large in comparison with the thickness of the layer. Howarth,[23] Frössling,[24] Scholkemeyer,[25] Tifford,[26] and others

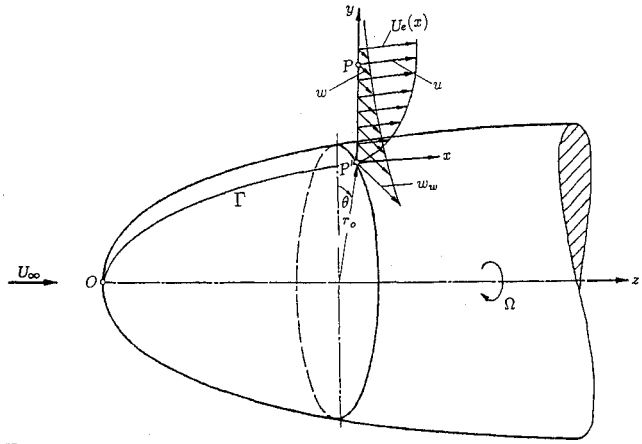

Fig. 1 Basic notations for boundary layer on a blunt-nosed cylinder.

obtained the boundary-layer solutions by employing the series method. In addition, Baxter et al.,[27] Raetz,[28] and Wu[29] applied explicit finite-difference procedures to solve this boundary-layer problem. For some boundary-layer problems, explicit methods are inherently unstable due to numerical instabilities. To obtain a stable and accurate solution, the idea of the Hartree-Womersley method[30] was applied to the incompressible boundary layer by Hartree,[31] Manohar,[32] and Smith and Clutter.[33] Adopted in this paper is an implicit finite-difference method accompanied with a fine mesh computational grid system near the body surface, which provides not only stable and accurate results but also a simpler procedure for obtaining the velocity profiles.

After the boundary-layer flow is computed, the Chebyshev collocation spectral method is employed to examine its stability behavior.

II. Analysis

In this section, a procedure is described for studying the stability of flow along a cylindrical blunt-nosed body of varying radius. The flow outside and that within the thin boundary layer are first computed, and then the stability behavior of the slightly perturbed boundary-layer flow is examined based on a linearized analysis.

Potential Flow Outside the Boundary Layer

In high Reynolds number flow past a streamlined body, the region outside the thin boundary layer is virtually a potential flow. The axisymmetric semi-infinitely long cylinder considered in this paper is a Rankine half-body, which is generated by superposition of a uniform flow of speed u_∞ in the direction of increasing z and a point source of strength m located at the origin. The stream function of the resulting flowfield is

$$\Psi = \frac{1}{2}u_\infty r^2 - m\left(1 + \frac{z}{\sqrt{r^2+z^2}}\right) \tag{1}$$

The body surface is represented by the streamline $\Psi = 0$, and its radius approaches the value $R_0 (= 2\sqrt{m/u_\infty})$ far downstream.

The velocity components are related to the stream function through the following equations:

$$u_r = -\frac{1}{r}\frac{\partial \Psi}{\partial z} = \frac{mr}{(r^2+z^2)^{3/2}} \tag{2a}$$

$$u_z = \frac{1}{r}\frac{\partial \Psi}{\partial r} = u_\infty + \frac{mz}{(r^2+z^2)^{3/2}} \tag{2b}$$

The total speed tangent to the body surface is taken as the speed at the edge of the boundary layer, which is computed as

$$u_e = \sqrt{(u_r^2 + u_z^2)_{\Psi=0}} \tag{3}$$

The pressure field can be computed from the steady Bernoulli equation. The pressure coefficient C_p is expressed as

$$C_p = \frac{p - p_\infty}{\frac{1}{2}\rho u_\infty^2} = 1 - \left(\frac{u_r}{u_\infty}\right)^2 - \left(\frac{u_z}{u_\infty}\right)^2 \tag{4}$$

Governing Equations in Curvilinear Coordinates

Considering the boundary-layer flow past a body of revolution, the curvilinear coordinates of a point P in space are designated (x, θ, y) as shown in Fig. 1. Using the transformations described in Ref. 34, the governing equations for the incompressible flow past a body of revolution can be described as

$$\frac{\partial u}{\partial t} + u\frac{\partial u}{\partial x} + \frac{w}{r_0}\frac{\partial u}{\partial \theta} + v\frac{\partial u}{\partial y} - \frac{w^2}{r_0}\frac{dr_0}{dx}$$

$$= -\frac{\partial p}{\partial x} + \frac{1}{Re_D}\left[\frac{\partial^2 u}{\partial x^2} + \frac{1}{r_0^2}\frac{\partial^2 u}{\partial \theta^2} + \frac{\partial^2 u}{\partial y^2}\right] \tag{5a}$$

$$\frac{\partial w}{\partial t}+u\frac{\partial w}{\partial x}+\frac{w}{r_0}\frac{\partial w}{\partial \theta}+v\frac{\partial w}{\partial y}+\frac{uw}{r_0}\frac{dr_0}{dx}$$
$$=-\frac{1}{r_0}\frac{\partial p}{\partial \theta}+\frac{1}{Re_D}\left[\frac{\partial^2 w}{\partial x^2}+\frac{1}{r_0^2}\frac{\partial^2 w}{\partial \theta^2}+\frac{\partial^2 w}{\partial y^2}\right] \quad (5b)$$

$$\frac{\partial v}{\partial t}+u\frac{\partial v}{\partial x}+\frac{w}{r_0}\frac{\partial v}{\partial \theta}+v\frac{\partial v}{\partial y}$$
$$=-\frac{\partial p}{\partial y}+\frac{1}{Re_D}\left[\frac{\partial^2 v}{\partial x^2}+\frac{1}{r_0^2}\frac{\partial^2 v}{\partial \theta^2}+\frac{\partial^2 v}{\partial y^2}\right] \quad (5c)$$

$$\frac{\partial (r_0 u)}{\partial x}+\frac{\partial w}{\partial \theta}+\frac{\partial (r_0 v)}{\partial y}=0 \quad (5d)$$

These equations are nondimensionalized with respect to the freestream velocity u_∞ and the downstream diameter D.

Laminar Boundary-Layer Equations

The basic notation and scheme of coordinates for the boundary layer on body of revolution are shown in Fig. 1. $U_e(x)=u_e/u_\infty$ is the dimensionless velocity in the x direction of the flow at the edge of the boundary layer. The body spins at a constant angular velocity Ω. Thus, for a particular station where the local radius is $\tilde{r}_0$, the dimensional tangential velocity at that station can be expressed as $\tilde{r}_0\Omega$. Since the motion is independent of θ, and under the assumption of thin boundary layer, the above governing equations are reduced to the boundary-layer equations of motion for steady flow,

$$u\frac{\partial u}{\partial x}+v\frac{\partial u}{\partial y}-\frac{w^2}{r_0}\frac{dr_0}{dx}=U_e\frac{dU_e}{dx}+\frac{1}{Re_D}\frac{\partial^2 u}{\partial y^2} \quad (6a)$$

$$u\frac{\partial w}{\partial x}+v\frac{\partial w}{\partial y}+\frac{uw}{r_0}\frac{dr_0}{dx}=\frac{1}{Re_D}\frac{\partial^2 w}{\partial y^2} \quad (6b)$$

$$\frac{\partial}{\partial x}(r_0 u)+\frac{\partial}{\partial y}(r_0 v)=0 \quad (6c)$$

which are identical to those obtained by Boltz[20] and Millikan.[21] With the subscript w denoting the wall, the boundary conditions at $y=0$ are

$$u_w=0$$
$$v_w=0 \text{ (impermeable wall)}$$
$$w_w=\frac{\tilde{r}_0\Omega}{u_\infty} \quad (7a)$$

and as

$$y\to\infty: \quad u=U_e(x), \qquad w=0 \quad (7b)$$

As mentioned in Ref. 1, for the forced flow with rotation, no similarity transformation can be found that can reduce the partial differential equations to ordinary ones. Nevertheless, a more convenient form is obtained for Eqs. (6a) and (6b) by introducing a stream function ψ and the following transformations

$$u=\frac{1}{r_0}\left(\frac{\partial r_0\psi}{\partial y}\right)=\frac{\partial \psi}{\partial y} \quad (8a)$$

$$v=-\frac{1}{r_0}\left(\frac{\partial r_0\psi}{\partial x}\right)=-\frac{\partial \psi}{\partial x}-\frac{\psi}{r_0}\frac{dr_0}{dx} \quad (8b)$$

$$\eta=y\left(\frac{U_\infty Re_D}{x}\right)^{1/2} \quad (8c)$$

$$\psi=\left(\frac{U_\infty x}{Re_D}\right)^{1/2}f(\eta) \quad (8d)$$

$$w=U_\infty g \quad (8e)$$

where $U_\infty=1$ is the dimensionless freestream velocity. Manipulating Eqs. (8a–8d) gives

$$u=U_\infty f' \quad (9a)$$

$$v=\frac{1}{2}\left(\frac{U_\infty}{xRe_D}\right)^{1/2}(\eta f'-f)-\left(\frac{U_\infty x}{Re_D}\right)^{1/2}\left(\frac{\partial f}{\partial x}+f\frac{1}{r_0}\frac{dr_0}{dx}\right) \quad (9b)$$

where a prime denotes differentiation with respect to η. Upon substitution of those expressions, the governing Eqs. (6a) and (6b) become

$$f'''=-\left(\frac{1}{2}+R\right)ff''-U_e^2M+x\left[f'\frac{\partial f'}{\partial x}-f''\frac{\partial f}{\partial x}\right]-Rg^2 \quad (10)$$

$$g''=-\left(\frac{1}{2}+R\right)fg'+x\left[f'\frac{\partial g}{\partial x}-g'\frac{\partial f}{\partial x}\right]+Rf'g \quad (11)$$

in which $R=(x/r_0)(dr_0/dx)$ and $M=(x/U_e)(dU_e/dx)$. A positive M represents a favorable pressure gradient and a negative M an adverse one. On any blunt body $M=R=1$ at the stagnation point as proved in Ref. 35. The boundary conditions are

$$\eta=0: \quad f_w'=0, \quad f_w=0, \quad g_w=\frac{w_w}{U_\infty}=\frac{\tilde{r}_0}{R_0}S \quad (12a)$$

as

$$\eta\to\infty: \quad f'=U_e, \quad g=0 \quad (12b)$$

The dimensionless spin rate $S(=R_0\Omega/u_\infty)$ is a measure of the far downstream tangential speed of the cylinder as compared to the reference axial speed. Note that the local spin rate g_w is equal to the downstream spin rate S multiplied by the ratio of the local and downstream radii.

The equations governing the flow around a nonspinning body are deduced by letting $g=0$ in Eqs. (10–12).

Linear Stability Theory

By introducing the following dimensionless variables

$$\xi=\frac{x}{\delta}, \quad \eta=\frac{y}{\delta}, \quad \zeta=\frac{r_0\theta}{\delta}, \quad \tau=\frac{t}{\delta/U_\infty}, \quad \delta=\left(\frac{x}{U_\infty Re_D}\right)^{1/2} \quad (13)$$

the governing Eqs. (5a–5d) are expressed as

$$\frac{\partial u}{\partial \tau}+u\frac{\partial u}{\partial \xi}+w\frac{\partial u}{\partial \zeta}+v\frac{\partial u}{\partial \eta}-\frac{R}{Re_\delta}w^2$$
$$=-\frac{\partial p}{\partial \xi}+\frac{1}{Re_\delta}\left[\frac{\partial^2 u}{\partial \xi^2}+\frac{\partial^2 u}{\partial \zeta^2}+\frac{\partial^2 u}{\partial \eta^2}\right] \quad (14a)$$

$$\frac{\partial w}{\partial \tau}+u\frac{\partial w}{\partial \xi}+w\frac{\partial w}{\partial \zeta}+v\frac{\partial w}{\partial \eta}+\frac{R}{Re_\delta}uw$$
$$=-\frac{\partial p}{\partial \zeta}+\frac{1}{Re_\delta}\left[\frac{\partial^2 w}{\partial \xi^2}+\frac{\partial^2 w}{\partial \zeta^2}+\frac{\partial^2 w}{\partial \eta^2}\right] \quad (14b)$$

$$\frac{\partial v}{\partial \tau}+u\frac{\partial v}{\partial \xi}+w\frac{\partial v}{\partial \zeta}+v\frac{\partial v}{\partial \eta}$$
$$=-\frac{\partial p}{\partial \eta}+\frac{1}{Re_\delta}\left[\frac{\partial^2 v}{\partial \xi^2}+\frac{\partial^2 v}{\partial \zeta^2}+\frac{\partial^2 v}{\partial \eta^2}\right] \quad (14c)$$

$$\frac{\partial u}{\partial \xi}+\frac{R}{Re_\delta}u+\frac{\partial w}{\partial \zeta}+\frac{\partial v}{\partial \eta}=0 \quad (14d)$$

in which the Reynolds number Re_δ is defined as $U_\infty\delta Re_D$. Re_δ and Re_D are related through the equation

$$Re_D=Re_\delta^2/xU_\infty \quad (15)$$

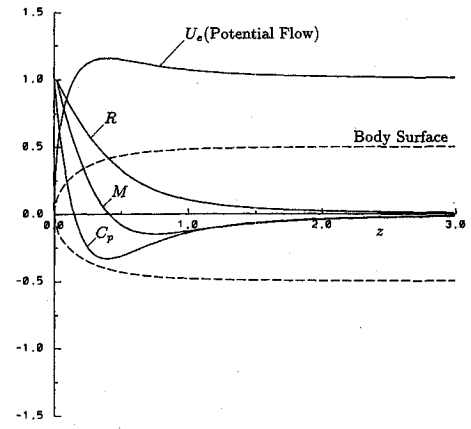

Fig. 2 Shape of body surface and the variations of U_e, R, C_p, and M in the axial direction.

We now suppose that the velocity V and pressure P in a laminar boundary layer on the rotating blunt-nosed cylinder is slightly perturbed. The resultant velocity and pressure are expressed by

$$v = V + v', \qquad p = \mathrm{P} + p' \tag{16}$$

Note that P is determined by the potential flow solution and V, having components (U,V,W), is the solution of Eqs. (6) expressed in dimensionless form. We shall take advantage of linearization and seek solutions of the type

$$u'(\xi,\eta,\zeta,\tau) = \hat{u}(\eta)\cdot\exp[i\alpha(\xi - c\tau) + in\zeta]$$

$$v'(\xi,\eta,\zeta,\tau) = \hat{v}(\eta)\cdot\exp[i\alpha(\xi - c\tau) + in\zeta]$$

$$w'(\xi,\eta,\zeta,\tau) = \hat{w}(\eta)\cdot\exp[i\alpha(\xi - c\tau) + in\zeta]$$

$$p'(\xi,\eta,\zeta,\tau) = \hat{p}(\eta)\cdot\exp[i\alpha(\xi - c\tau) + in\zeta] \tag{17}$$

Substituting Eqs. (17) into Eqs. (16) and (14) and invoking Eqs. (6), we obtain a system of ordinary differential equations

$$(U-c)\hat{u} + \frac{nW}{\alpha}\hat{u} - \frac{iU'}{\alpha}\hat{v} + \frac{i2RW}{\alpha Re_\delta}\hat{w} + \hat{p}$$

$$+\frac{i}{\alpha Re_\delta}[\hat{u}'' - (\alpha^2 + n^2)\hat{u}] = 0 \tag{18a}$$

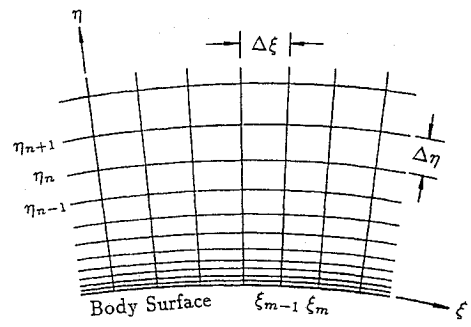

Fig. 3 Schematic of the computational grid system.

$$(U-c)\hat{w} + \left(\frac{nW}{\alpha} - \frac{iRU}{\alpha Re_\delta}\right)\hat{w} - \frac{iRW}{\alpha Re_\delta}\hat{u} - \frac{iW'}{\alpha}\hat{v}$$

$$+\frac{n}{\alpha}\hat{p} + \frac{i}{\alpha Re_\delta}[\hat{w}'' - (\alpha^2 + n^2)\hat{w}] = 0 \tag{18b}$$

$$(U-c)\hat{v} + \frac{nW}{\alpha}\hat{v} - \frac{i}{\alpha}\hat{p}' + \frac{i}{\alpha Re_\delta}[\hat{v}'' - (\alpha^2 + n^2)\hat{v}] = 0 \tag{18c}$$

$$\left(1 - \frac{iR}{\alpha Re_\delta}\right)\hat{u} + \frac{n}{\alpha}\hat{w} - \frac{i}{\alpha}\hat{v}' = 0 \tag{18d}$$

The no-slip boundary condition at the wall requires that $\hat{u} = \hat{v} = \hat{w} = 0$ at $\eta = 0$. At the outer boundary conditions, it is stated that $\hat{u}$, $\hat{v}$, $\hat{w} \to 0$ at a height far from the wall instead of at the edge of the boundary layer, because the spiral vortices of small wave numbers may grow beyond the outer edge of the boundary layer. Therefore, the boundary conditions are written as follows:

$$\eta = 0: \qquad \hat{u} = \hat{v} = \hat{w} = 0 \tag{19a}$$

as

$$\eta \to \infty: \qquad \hat{u} = \hat{v} = \hat{w} = \hat{p} = 0 \tag{19b}$$

III. Method of Solution

The solution of Eqs. (10) and (11) is made difficult by both the nonlinearity and the fact that one boundary condition is at $\eta = \infty$. Discussed in Ref. 1 is a method of solution that involves choosing values of f_w'' and g_w' and integrating the equations directly up to a selected large value of η, which requires that the values of f' and g remain within certain bounds. Calculations are accomplished by satisfying the outer boundary conditions within a specified tolerance, typically of order 10^{-6}.

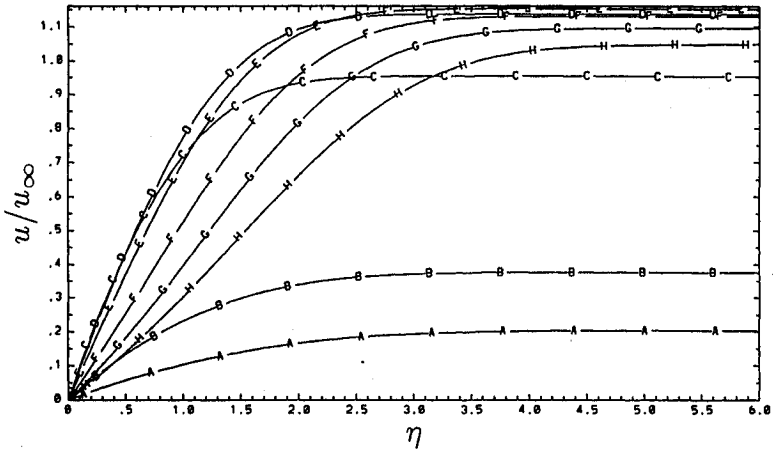

Fig. 4 Meridional velocity profiles for the flow over nonspinning Rankine nose cylinder; A: $x = 0.05$, B: $x = 0.095$, C: $x = 0.305$, D: $x = 0.5$, E: $x = 0.605$, F: $x = 0.8$, G: $x = 0.995$, H: $x = 1.4$.

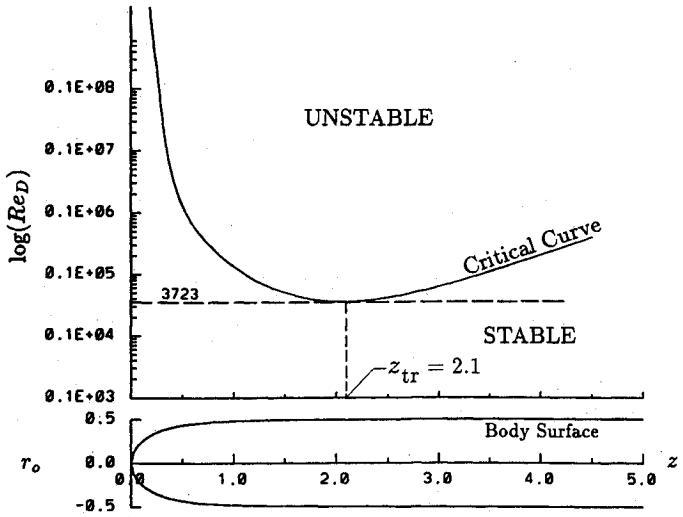

Fig. 5 Critical curve for nonspinning Rankine nose cylinder; the most unstable mode is $n = 0$ at all locations.

Table 1 Positions of onset of instability and critical Reynolds numbers

S	z_{tr}	$(Re_D)_{crit}$
0.00	2.10	3723
0.05	1.94	3032
0.10	1.85	2574
0.20	1.78	1930
0.60	1.38	762

Once the mean flowfield has been obtained, the efficient Chebyshev collocation spectral method, which provides accurate results, is then applied to solve the complex eigenvalue problem concerning its hydrodynamic instability. This numerical technique and its procedure have been described in detail in Ref. 1.

IV. Results and Discussion

Following the computational procedures described previously for the stability of laminar boundary layers, results have been obtained for a cylinder of given shape with and without a spin motion about its axis.

Nonspinning Body

A numerical example is presented for a Rankine nose body, whose geometry as well as the variations in z of the potential velocity U_e, the pressure gradient M, the radius parameter R, and the pressure coefficient C_p is shown in Fig. 2. It is noted that the potential velocity accelerates starting from the stagnation point, reaches a maximum value on the blunt nose, and then decelerates gradually and finally returns to the reference velocity U_∞. This velocity distribution causes a favorable pressure gradient with positive values of M in the region $0 \le x \le 0.43$ near the nose, which is followed by an adverse pressure gradient with negative values of M.

Figure 3 illustrates the schematic of the computational grid system used for solving Eqs. (10–12) for the velocity field in the boundary layer. The fine-size mesh near the wall ensures an accurate result of the calculation within the boundary layer. Figure 4 shows the meridional velocity profiles at different stations along the cylinder. Inflection points appear in the profiles plotted in the region $x > 0.43$ of adverse pressure gradient.

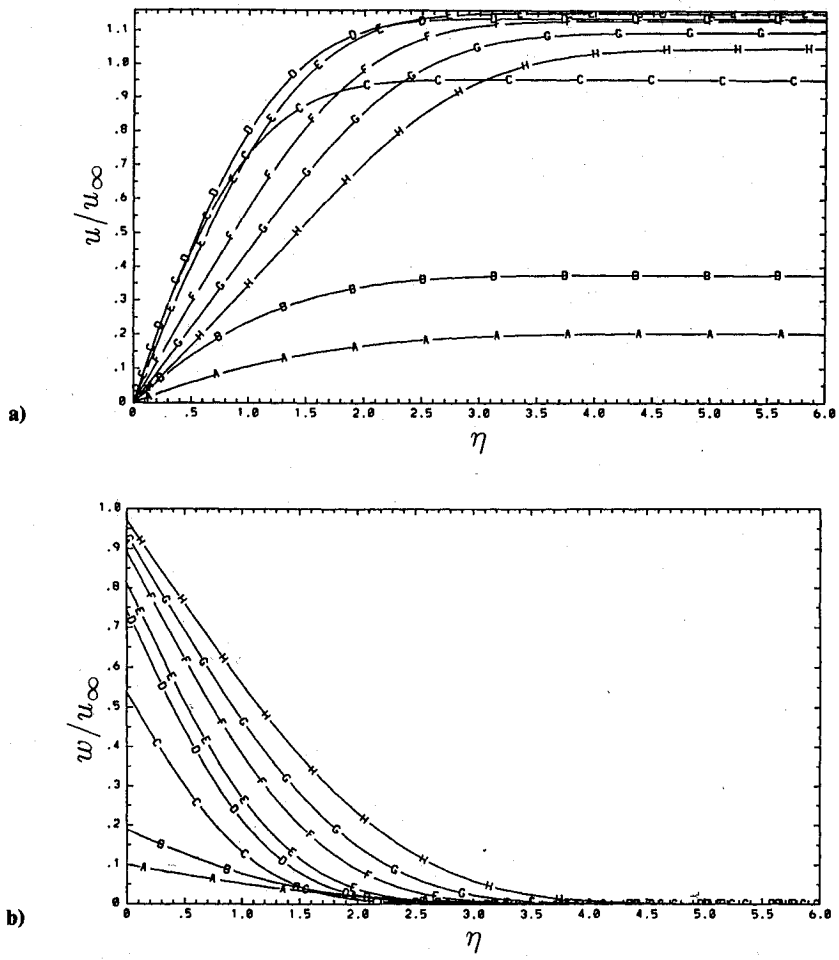

Fig. 6 Velocity profiles for the flow over spinning Rankine nose cylinder with $S = 1$ at stations denoted by the same symbols shown in Fig. 4: a) meridional velocity, b) tangential velocity.

The study is continued to predict the critical conditions for the instability of an axisymmetric boundary layer with the combined influence of transverse curvature and pressure gradient. By solving the complex eigenvalue system of Eqs. (18a–18d) with the boundary conditions of Eqs. (19a) and (19b), for given n and x, a correct eigensolution is obtained when a combination of the three dimensionless parameters α, Re_δ, and c is found which satisfies those equations. In some cases, the viscous theories verify the existence of an unstable region in which infinitesimal disturbances are amplified (with $c_i > 0$). The boundary of this region is the so-called neutral stability curve for a given mode n, which is the locus of $c_i = 0$. The lowest Reynolds number to which the neutral stability curves for all modes n protrude is called the critical Reynolds number; typically the inflection profile has a smaller critical value. For given α and Re, the computating time was found to be approximately 0.2 s on a Cyber 205 to obtain the eigenvalues and eigenfunctions.

A computational result of the critical Reynolds numbers Re_D along the body surface is shown in Fig. 5. The relation between Re_δ and Re_D has been described in Eq. (15). It is found that, for such a Rankine nose body, the axisymmetric disturbance ($n = 0$) prompts a most unstable situation at all locations of z, which causes the onset of transition to appear in the form of a two-dimensional Tollmien-Schlichting wave. As indicated in Fig. 5, onset of instability occurs at $z_{tr} = 2.1$ within the region of adverse pressure gradient where there is a lowest critical Reynolds number $Re_D = 3723$. This is also the region where the two-dimensional waves were observed experimentally in the smoke pictures for all but the very low Reynolds number flows. This computed location of onset of instability is comparable to the value of about 2.7 reported in Ref. 16 for a tangent-ogive nose cylinder based on laboratory observations. Evidently, the onset of instability region moves upstream with increasing Reynolds number.

Spinning Body

The distributions of both meridional and tangential velocities, obtained by solving Eqs. (10) and (11) with the boundary conditions of Eqs. (12a) and (12b) for a spin rate of $S = 1$, are shown in Figs. 6a and 6b at different x stations. A comparison of Fig. 6a with Fig. 4 reveals that the meridional velocity profiles are made slightly fuller by introducing the spin motion. Similar to the nonspinning body, inflection profiles are again obtained in the region of adverse pressure gradient.

Upon completion of stability computations, the results are presented for cases to cover a range of Reynolds numbers, wave numbers, and spin rates. Experimental evidence that the spin motion destabilizes the flow is confirmed by the present

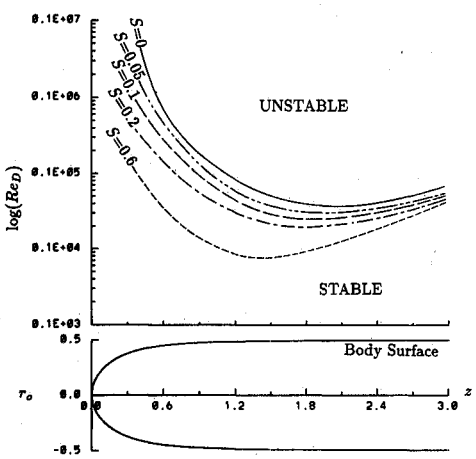

Fig. 7 Comparison of critical curves for various values of spin rate; the most unstable mode for $S = 0$, 0.05, 0.1, and 0.2 is $n = 0$ at all locations, and that for $S = 0.6$ is $n = 2$ for z up to about 2.34, and changes to $n = 3$ thereafter.

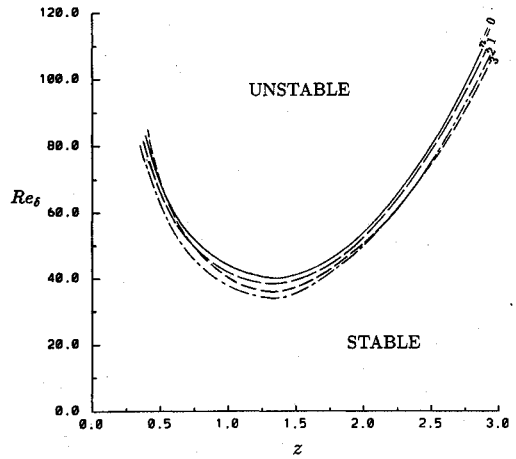

Fig. 8 Neutral stability curves for axisymmetric and nonaxisymmetric disturbances with dimensionless spin rate $S = 0.6$.

calculations, as shown in Fig. 7. It is of interest to note that, for low spin rates with $S = 0$, 0.05, 0.1, and 0.2 in Fig. 7, as in the nonspinning case, the onset of transition is first excited by axisymmetric disturbance ($n = 0$), which is in agreement with wind-tunnel observations.[16]

As for a fast spin motion with $S = 0.6$, Fig. 8 illustrates the critical Reynolds numbers for $n \leq 3$. It is found that, for a given z, each mode has its own critical Reynolds number. The lowest among all of those critical values is the critical Reynolds number of the boundary layer at that particular z, which is represented by the lower envelope of all curves. Note that the most unstable mode varies along z; it remains at $n = 2$ from the front nose region for z to around 2.34, and changes to $n = 3$ as z increases further, and so forth.

The critical Reynolds number Re_D vs z curve for a spin rate of $S = 0.6$ can be found in Fig. 7. The plot shows that a minimum value of $Re_D = 762$ is required to make the boundary layer unstable at the distance $z_{tr} = 1.38$; $n = 2$ is the mode to be amplified. Table 1 lists the positions of onset of instability and the corresponding critical Reynolds numbers for different values of spin rate. It is encouraging that the computed results are in qualitative agreement with the observations for spin rates greater than 0.4, which indicate that an inflectional cross-flow instability generates spiral vortices around the body, which yields a striated appearance of the smoke in the boundary layer. A quantitative comparison with experiment is not possible because of the lack of experimental data on spinning bodies of the shape described in the present analysis.

As a result of increased spin rate for a given freestream velocity, the location of onset of instability shifts upstream toward the front nose region, and the critical Reynolds number decreases. On the other hand, for a constant spin motion, the instability zone moves forward with a decreasing Reynolds number because of the corresponding increase of S, which is opposite to what occurred on the nonspinning model.

V. Conclusions

Numerical techniques have been developed successfully to study the stability of boundary layers on nonspinning and spinning Rankine nose cylinders, with the axis of symmetry parallel to the oncoming flow. Onset of transition is first excited in the unstable region (which is usually the adverse pressure gradient region) by the two-dimensional Tollmien-Schlichting wave on a nonspinning body. With slow spin motions, the first mode of instability resembles that of a two-dimensional wave observed on the nonspinning model. However, with fast spin motions, results show that nonaxisymmetric disturbances are amplified instead, which is in agreement with experimental observations.

This paper provides the computations for the stability of axisymmetric boundary layers on a blunt-nosed cylinder under

the influences of transverse curvature and spin motion. Further investigations can be pursued by including the effects of compressibility and nose shape, for example. For the case in which the body is at an angle of attack, the present theory has to be modified to examine the stability of a nonaxisymmetric boundary layer.

Acknowledgments

The authors are grateful to E. Laurien for his valuable advice and discussion on the application of Chebyshev collocation spectral method. This work was sponsored by the Air Force Office of Scientific Research under Contract F49620-88-C-0098. Part of the work of the first author was supported by NASA Lewis Research Center under Grant NCC3-168. The U.S. Government is authorized to reproduce and distribute reprints for governmental purposes notwithstanding any copyright notation hereon.

References

[1]Kao, K. H., and Chow, C. Y., "Stability Analyses of Boundary Layer on a Semi-Infinite Circular Cylinder With and Without Spin," AIAA Paper 90-0116, Jan. 1990.

[2]Schubauer, G. B., and Skramstad, H. K., "Laminar Boundary Layer Oscillations and Stability of Laminar Flow," *Journal of the Aeronautical Sciences,* Vol. 14, Feb. 1947, pp. 69–78; see also NACA Rept. 909, 1947.

[3]Liepmann, H. W., "Investigation of Boundary Layer Transition on Concave Walls," NACA Wartime Rept., ACR4J28, Vol. W87, 1945.

[4]Pretsch, J., "Die Stabilität einer ebenen Laminarströmung bei Druckgefälle und Druckansteig," *Jahrbuch der Deutschen Luftfahrtforschung,* Vol. 1, Oct. 1941, pp. 158–175.

[5]Pretsch, J., "Die Anfachung instabiler Störungen in einer laminaren Reibungsschicht," *Jahrbuch der Deutschen Luftfahrtforschung,* Vol. 2, April 1942, pp. 154–171. (Translated as "The excitation of unstable perturbations in a laminar friction layer," NACA TM-1343.)

[6]Hahnemann, E., Freeman, J. C., and Finston, M., "Stability of Boundary Layers and of Flow in Entrance Section of Channel," *Journal of the Aeronautical Sciences,* Vol. 15, Aug. 1948, pp. 493–496.

[7]Tetervin, N., "A Study of the Stability of the Incompressible Boundary Layer on Infinite Wedges," NACA TN-2976, 1953.

[8]Schlichting, H., and Ulrich, A., "Zur Berechung des Unischlages laminar/turbulent," *Lilienthal-Gesellschaft fur Luftfahrtforschung,* Berlin, Vol. S10, 1940, pp. 75–135; and *Jahrbuch der Deutschen Luftfahrtforschung,* Vol. 2, Jan. 1942, pp. 8–35.

[9]Tetervin, N., and Levine, D. A., "A Study of the Stability of the Laminar Boundary Layer as Affected by Changes in the Boundary-Layer Thickness in Regions of Pressure Gradient and Flow Through the Surface," NACA TN-2752, 1952.

[10]Kobayashi, R., Kohama, Y., and Kurosawa, M., "Boundary Layer Transition on a Rotating Cone in Axial Flow," *Journal of Fluid Mechanics,* Vol. 127, Feb. 1983, pp. 341–352.

[11]Sawatzki, O., "Das Strömungsfeld um eine rotierende Kugel," *Acta Mechanica,* Vol. 9, 1970, pp. 159–214.

[12]Wimmer, M., "Experimentelle Untersuchungen der Strömung im Spalt zwischen zwei konzentrischen Kugeln, die beide um einen gemeinsamen Durchmesser rotieren," Diss., Fakultät für Masch. der Univ. Karlsruhe (TH), Karlsruhe, Germany, 1974.

[13]Kohama, Y., and Kobayashi, R., "Boundary Layer Transition and the Behavior of Spiral Vortices on Rotating Spheres," *Journal of Fluid Mechanics,* Vol. 137, Dec. 1983, pp. 153–164.

[14]Brown, F. N. M., "The Physical Model of Boundary Layer Transition," *Ninth Midwestern Mechanics Conference,* Univ. of Wisconsin Press, Madison, WI, 1965.

[15]Knapp, C. F., and Roache, P. J., "A Combined Visual and Hot-Wire Anemometer Investigation of Boundary-Layer Transition," *AIAA Journal,* Vol. 6, No. 1, Jan. 1968, pp. 29–36.

[16]Kegelman, J. T., Nelson, R. C., and Mueller, T. J., "Boundary Layer and Side Force Characteristics of a Spinning Axisymmetric Body," AIAA Paper 80-1584, Aug. 1980.

[17]Kegelman, J. T., Nelson, R. C., and Mueller, T. J., "The Boundary Layer on an Axisymmetric Body with and without Spin," *AIAA Journal,* Vol. 21, No. 11, 1983, pp. 1485–1491.

[18]Kohama, Y., "Flow Structures Formed by Axisymmetric Spinning Bodies," *AIAA Journal,* Vol. 23, No. 9, 1985, pp. 1445–1447.

[19]Stetson, K. F., "On Cone Frustum Pressure Gradient Effects on Transition," *AIAA Journal,* Vol. 26, No. 4, 1988, pp. 500–502.

[20]Boltz, E., "Grenzschichten an Rotationskörpern in Flüssigkeiten mit kleiner Reibung," Dissertation, Göttingen, Germany, 1908.

[21]Millikan, C. B., "The Boundary Layer and Skin Friction for a Figure of Revolution," *Transactions of the American Society of Mechanical Engineers (Applied Mechanics Section),* Vol. 54, Jan. 1932, pp. 29–43.

[22]Mangler, W., "Boundary Layers with Symmetrical Airflow About Bodies of Revolution," Goodyear Aircraft Corp. Translation, Rept. R-30-18, Pt. 20, 1945.

[23]Howarth, L., "On the Solution of the Laminar Boundary Layer Equations," *Proceedings of the Royal Society,* London, Vol. A164, 1938, pp. 547–558.

[24]Frössling, N., "Verdunstung, Wärmeübergang und Geschwindigkeitsverteilung bei zwei-dimensionaler und rotationssymmetrischer laminarer Grenzschichtströmung," Lunds Universitets Arsskrift, Lund, Sweden, Vol. 2, No. 4, 1940, p. 35.

[25]Scholkemeyer, F. W., "Die laminare Reibungsschicht an rotationssymmetrischen Körpern," Dissertation, Braunschweig, 1943; see also *Archiv der Mathematik,* Vol. 1, No. 4, 1949, pp. 270–277.

[26]Tifford, A. N., "Heat Transfer and Frictional Effects in Laminar Boundary Layers. Part 4. Universal Series Solutions," Wright Air Dev. Center TR 53-288, Aug. 1954.

[27]Baxter, D. C. and Flügge-Lotz, I., "The Solution of Compressible Laminar Boundary Layer Problems by a Finite Difference Method. Part 2. Further Discussion of the Method and Computation of Examples," Stanford Univ. Division of Engineering Mechanics, TR 110, ASTIA 148080, Oct. 15, 1957; see also *Zeitschrift fur Angewandte Mathematik und Physik,* Vol. 9b, 1958, pp. 81–90.

[28]Raetz, G. S., "A Method of Calculating the Incompressible Laminar Boundary Layer on Infinitely-Long Swept Suction Wings, Adaptable to Small-Capacity Automatic Computers," Northrop Aircraft Co., Los Angeles, CA, Rept. BLC-11, Sept. 1953.

[29]Wu, J. C., "The Solution of the Laminar Boundary Layer Equations by the Finite Difference Method," *Proceeding of the 1961 Heat Transfer and Fluid Mechanics Institute,* Stanford Univ. Press, Stanford, CA, 1962, pp. 55–69.

[30]Hartree, D. R., and Womersley, J. R., "A Method for the Numerical or Mechanical Solution of Certain Types of Partial Differential Equations," *Proceedings of the Royal Society,* London, Vol. A101, Aug. 1937, pp. 353–366.

[31]Hartree, D. R., "The Solution of the Equation of the Laminar Boundary Layer for Schubauer's Observed Pressure Distribution for an Elliptic Cylinder," British Aeronautical Research Council, R&M No. 2427, April 1949.

[32]Manohar, R., "A Characteristic Difference Method for the Calculation of Steady Boundary-Layer Flow," *Proceeding of the 4th Congress of Theoretical Applied Mechanics,* Indian Society of Theoretical Applied Mechanics, Kharagpur, India, 1958, pp. 135–144.

[33]Smith, A. M. O., and Clutter, D. W., "Solution of the Incompressible Laminar Boundary-Layer Equations," *AIAA Journal,* Vol. 1, No. 9, Sept. 1963, pp. 2062–2071.

[34]Schlichting, H., "Über die theoretische Berechung der kritischen Reynoldsschen Zahl einer Reibungsschicht in beschleunigter und verzögerter Strömung," *Jahrbuch der Deutschen Luftfahrtforschung,* Vol. 1, 1940, pp. 97–112.

[35]Smith, A. M. O., and Clutter, D. W., "Solution of the Incompressible Laminar Boundary-Layer Equations," Douglas Aircraft Co., Long Beach, CA, Rept. ES 40446, July 1961.

Walter B. Sturek
Associate Editor